Journal of Applied Polymer Science

Photosensitive antibacterial and cytotoxicity performances of a TiO_2/carboxymethyl chitosan/poly(vinyl alcohol) nanocomposite hydrogel by *in situ* radiation construction

Yue-Sheng Li,[1] Yan Han,[2] Jiang-Tao Qin,[3] Zhi-Yong Song,[1] Hua-Hua Cai,[4] Ji-Fu Du,[1] Shao-Fa Sun,[1] Yi Liu[2]

[1]Nonpower Nuclear Technology Collaborative Innovation Center, Hubei University of Science and Technology, Xianning 437100, People's Republic of China

[2]State Key Laboratory of Virology and Key Laboratory of Analytical Chemistry for Biology and Medicine (Ministry of Education), College of Chemistry and Molecular Sciences, Wuhan University, Wuhan 430072, People's Republic of China

[3]College of Life and Environmental Sciences, Shanghai Normal University, Shanghai 200234, People's Republic of China

[4]Tongji Medical College, Huazhong University of Science and Technology, Wuhan 430000, People's Republic of China

Correspondence to: Y. Liu (E-mail: yiliuchem@whu.edu.cn)

ABSTRACT: Nano-TiO_2/carboxymethyl chitosan (CMCS)/poly(vinyl alcohol) (PVA) ternary nanocomposite hydrogels were prepared by freezing–thawing cycles and electron-beam radiation with PVA, CMCS, and nano-TiO_2 as raw materials. The presence of nano-TiO_2 nanoparticles in the composite hydrogels was confirmed by thermogravimetry, Fourier transform infrared spectroscopy, and X-ray powder diffraction. Field emission scanning electron microscopy images also illustrated that the TiO_2/CMCS/PVA hydrogel exhibited a porous and relatively regular three-dimensional network structure; at the same time, there was the presence of embedded nano-TiO_2 throughout the hydrogel matrix. In addition, the nano-TiO_2/CMCS/PVA composite hydrogels displayed significant antibacterial activity with *Escherichia coli* and *Staphylococcus aureus* as bacterial models. The antibacterial activity was demonstrated by the antibacterial circle method, plate count method, and cell density method. Also, with the Alamar Blue assay, the cytotoxicity of the composite hydrogel materials to L929 cells was studied. The results suggest that these materials had no obvious cytotoxicity. Thus, we may have developed a novel, good biocompatibility hydrogel with inherent photosensitive antibacterial activity with great potential for applications in the fields of cosmetics, medical dressings, and environmental protection. © 2016 Wiley Periodicals, Inc. J. Appl. Polym. Sci. **2016**, *133*, 44150.

KEYWORDS: biomaterials; crosslinking; irradiation; microgels; nanostructured polymers

Received 23 December 2015; accepted 29 June 2016
DOI: 10.1002/app.44150

INTRODUCTION

Hydrogels are three-dimensional, hydrophilic, polymeric networks that are able to absorb large amounts of water or biological fluids.[1] The networks are insoluble because of the presence of chemical crosslinks (tie points, junctions) or physical crosslinks. Although hydrogels contain a large amount of water, they can display a certain shape as a solid and have very important research and application value as antibacterial dressings.[2] These studies show that hydrogel composite materials have good antibacterial properties against Gram-positive bacteria (e.g., *Staphylococcus aureus*) and Gram-negative bacteria (*Escherichia coli*).[3–8] Furthermore, antimicrobial agents can be combined within hydrogels without impairments in their bioactivity; this may result in advantages of sustainable release of antibacterial.[9]

Chitosan is a polysaccharide derived from chitin; it exhibits numerous interesting physicochemical and biological properties.[10] Compared with other water-soluble chitosan derivatives, carboxymethyl chitosan (CMCS) has been widely studied because of its ease of synthesis, ampholytic characteristics, and the possibilities of ample applications.[11] Currently, a lot of studies have been focused on developing chitosan composite hydrogels with good antibacterial properties.[12–16] Moreover, Radhakumary *et al.*[17] used modified poly(N-isopropyl acrylamide) chitosan as a carrier, mixed it with ciprofloxacin, prepared a temperature-sensitive gel dressing with antibacterial and drug-releasing properties. Vimala *et al.*[18] prepared porous silver chitosan nanocomposite thin films, which had excellent antibacterial properties because of their synergistic effect. As an important component of antibacterial dressing, CMCS has received much attention.

Poly(vinyl alcohol) (PVA) is a kind of water-soluble polymer with a good hydrophobicity, biocompatibility, and degradation properties.[19] Because of its high water content, low toxicity, good biocompatibility, and easy processing properties, PVA has been widely used in biomedical[20] and biochemical applications.[21] At present, research into PVA as an important antibacterial hydrogel matrix material has also been reported. Juby *et al.*[22] synthesized a PVA–gum acacia–Ag composite hydrogel by a one-step method, and the composite hydrogel had good antibacterial properties against *E. coli*. Varaprasad *et al.*[23] synthesized an antibacterial nano-Ag composite material, which was based on polyacrylamide and PVA composite gel and effective in wound healing.

At present, nano-TiO_2 has become one of the hot spots in the field of antibacterial materials because they are chemically stable, biocompatible, and antibacterial.[24] On the basis of the previous advantages, nano-TiO_2 materials are widely used as an insecticides for automatic sterilization and disinfection on wall and floor tiles in the indoor environments of hospitals and other public places.[25] In fact, many studies have shown that nano-TiO_2 has broad-spectrum biocidal activity toward both Gram-positive and Gram-negative bacteria, such as *Bacillus subtilis*,[26] *Pseudomonas aeruginosa*,[27] and *E. coli*.[28] The addition of nano-TiO_2 to coatings can produce a sterilization, antifouling, deodorant, self-clean antibacterial, antifouling paint, which can be applied in the hospital ward, operation room, family bathroom, and other bacterially intensive, easy breeding places. These nanomaterials can purify the air, prevent infection, deodorize, and effectively kill harmful bacteria.[29,30]

In recent years, polymer/inorganic oxide composite hydrogel materials have attracted much attention. Young[31] prepared Ag–TiO_2–chitosan composites film by an electrochemical method, and and this film showed good antibacterial properties. Wen *et al.*[32] introduced nano-TiO_2 into the chitosan membrane, and this improved the wet strength of the film and the antibacterial properties. Dong *et al.*[33] introduced different contents of nano-TiO_2 into chitosan and the gelatin polymer matrix. They found that the resistance and toughness of the composite matrix were greatly improved so that the hybrid film was expected to become a new type of green antibacterial food-packaging material. Schwartz *et al.*[34] studied the antibacterial properties of a poly(N-isopropyl acrylamide) hydrogel coated with nano-ZnO. The results show that the composite hydrogel had good antibacterial properties for *E. coli*. Sahiner[35] reviewed the advantages of a radiation preparation method of a composite hydrogel; the excellent properties and potential applications in the field of this antibacterial hydrogel dressing were also discussed in detail.

However, the single component of the polymer hydrogel and the inorganic antibacterial agent (especially in terms of the mechanical properties and environmental response) have many shortcomings in practical applications; this greatly limits the application of functional materials in various fields. At present, there have been few reports on the preparation of polymer/inorganic nanocomposite hydrogel antibacterial materials by *in situ* radiation technology. In this study, we constructed nano-TiO_2/CMCS/PVA composite hydrogels *in situ* by electron-beam radiation, a freezing–thawing method, and other technical means. These methods are facile and controlled without the addition of any crosslinking agent. The antibacterial activity on *E. coli* and *S. aureus* and cytotoxicity on mouse skin fibroblasts (L929 cells) of the TiO_2/CMCS/PVA composite hydrogels was studied. The preparation of the composite hydrogels was carried out at room temperature; moreover, the reaction process did not require the addition of any toxic substances, so this was a green, environmentally friendly composite hydrogel preparation method. Also, the prepared hydrogels had a good crosslinking degree and a high purity. Our research was aimed to achieve a comprehensive balance of polymer and nano-inorganic material components in the performance, to eliminate the weakness of a single component in the performance, to obtain a more comprehensive performance of composite hydrogel antibacterial materials, and also to enrich and complement the application of composite hydrogels in the field of water gel antibacterial medical dressings. It has a very important scientific significance.

EXPERIMENTAL

Experimental Materials and Reagents

The following materials were used in the experiments: CMCS (chemically pure, Sinopharm Group Reagent Co., Ltd.); nano-TiO_2 (chemically pure, P25, Germany Degussa, Pu Shan Shanghai Chemical Co., Ltd.); PVA (1750 ± 50, Sinopharm Chemical Reagent Co., Ltd.); and Alamar Blue, 1640 fetal bovine serum, peptone, yeast extract, and beef extract (Sigma Co.). Strains of *E. coli* (CCTCCAB91112) and *S. aureus* (CCTCCAB910393) were obtained from Wuhan University (China) from a typical culture collection center. L929 cells were provided by Tongji Medical College. The Luria–Bertani culture medium contained sodium chloride (2.5 g), peptone (5 g), and yeast powder (2.5 g), which were dissolved in 500 mL of secondary water; it was kept at a pH of 7.0 and 120 °C, put under 1.034×10^5 Pa of pressure, and sterilized for 30 min. The nutrient broth medium components were sodium chloride (1 g), peptone (2 g), and beef extract (1.2 g), which were dissolved in 200 mL of secondary water; it was kept at pH 7.0 and 120 °C, put under 1.034×10^5 Pa of pressure, and sterilized for 30 min.

Experimental Apparatus

A JJ-1 force electric blender (Shandong City of Heze Province Biochemical Instrument Factory), a pure water machine (Wuhan Victor Wong Instrument Equipment Co., Ltd.); a vacuum-drying box (Shanghai Constant Scientific Instruments Co., Ltd.), a drying oven (Shanghai Constant Scientific Instruments Co., Ltd.), a DTDN series of ultrasonic cleaning machines (Ningbo Xinzhi Biological Polytron Technologies, Inc.), and an electronic balance (Shanghai Sunny Instruments) were used. X-ray powder diffraction (XRD) measurements were performed in the reflection mode (Cu Kα radiation, $\lambda = 1.5418$ Å) on a D8X Advance X-ray diffractometer; thermogravimetry (TG) was supported by Netzsch Scientific Instruments Co., Ltd. The morphology and particle sizes were determined with field emission scanning electron microscopy (FESEM; JSM-6700F, JEOL) and scanning electron microscopy (SEM; VEGA-3 SBH, Tescan, Czech Republic). IR spectra were recorded on a PerkinElmer Spectrum 2000 Fourier transform infrared (FTIR)

spectrometer. We also used a THZ-C-1 desktop frozen constant-temperature oscillator (Taicang City Experimental Equipment Factory), a RTAC-2 colony counter (Hefei Colony Counter-Tech Electronics Co., Ltd.), and a YXQ-LS-18SI automatic portable sterilizer (Shanghai Boxun Industrial Co., Ltd., a medical equipment factory), a fluorescent spectrophotometer (960 MC/CRT, shanghai INESA Analytical Instrument Co., Ltd.), a biological microscope (XSP-2CA, Shanghai Bimu Instrument Co., Ltd.), and a 1-MeV electron accelerator (Wasik Associates).

Preparation of the Nano-TiO_2/CMCS/PVA Composite Hydrogels

A certain mass of PVA particles was weighed accurately and placed in a three-necked flask. Then, a certain volume of distilled water as the solvent as added. The mixture was heated to 85 °C and stirred continuously for 2 h at a stirring rate 150 rpm so that the PVA particles were fully dissolved to prepare a 10% PVA aqueous solution and allowed to stand for 2 h to remove the bubble. An amount of 0.1 g of nano-TiO_2 was added to 25 mL of deionized water and exposed to ultrasound for 30 min; after the addition of 0.5 g of CMCS, the mixture was stirred continuously for 30 min to make the CMCS dissolve fully. Then, the PVA solution was added to the CMCS solution, and the mass ratio of TiO_2/CMCS/PVA was 1:5:20. After the solution was fully mixed and added to a 60-mm culture dish, a film 3 mm in thickness was prepared.

Nano-TiO_2/CMCS/PVA ternary composite hydrogel films 3 mm in thickness were placed in the freezer for 1 h, pump-vacuumed for 15 min, and moved to room temperature. The samples were thawed in a $60 \times 80\ mm^2$ plastic film bag; then, they were irradiated. The irradiation conditions were as follows: irradiation by an electron beam at doses of 30 kGy (1 Gy = 1 J/kg) at a dose rate of 100 kGy/s at room temperature with a 1-MeV electron accelerator, a voltage of 750 keV, a beam current of 10 mA; that is, the nano-TiO_2/CMCS/PVA composite hydrogel was prepared. Composite hydrogels with different swelling properties and mechanical strengths and porous and regular microstructures were obtained easily by electron beam; when the radiation or radiation dose rate was adjusted, it was easy to obtain a higher antibacterial activity of hydrogels. The hydrogel was soaked in distilled water for 48 h two times a day the first time. The obtained hydrogel was dried *in vacuo* for 2 h at 80 °C and then for 6 h at 60 °C to obtain the pure dry gel. When the content of TiO_2 was changed (from 0.5 to 6%, viz., 0.5, 1, 2, 3, 4, 5, and 6%), different TiO_2/CMCS/PVA composite hydrogels were obtained. In a manner similar to the previous approach, a CMCS/PVA composite hydrogel (mass ratio = 1:4) and TiO_2/PVA composite hydrogel (mass ratio = 1:20) were also prepared to compare with the TiO_2/CMCS/PVA ternary composite hydrogel. When the content of TiO_2 (5%) was fixed, several ternary composite hydrogels were also prepared at different mass ratios of CMCS to PVA (CMCS–PVA = 1:1, 1:2, 1:3, 1:4, 1:5, 1:6, 1:7, and 1:8).

Determination of the Antibacterial Properties of the Hydrogels

Suppression Loop Method. The culture medium solution containing the suspension of the tested bacteria was transferred to a culture dish, and the static distribution was uniform. A pie-shaped hydrogel was placed above the dish (1 cm in diameter) and then incubated for 24 h in a constant-temperature culture. Then, we used Vernier calipers to measure the inhibition zone diameter, and each sample was examined in three parallel experiments. Finally, according to eq. (1), we calculated the inhibition circle diameter:

$$W = (T - D)/2 \quad (1)$$

where W is the diameter of the antibacterial circle (mm), T is the total diameter of the sample and the antimicrobial circle (mm), and D is the diameter of the sample (mm).

Plate Count Method. The hydrogel sheet was transferred to the Petri dish, and we delineated a circular area in the hydrogel. A volume of 1 mL of bacterial medium was taken and uniformly coated on the surface of the hydrogel with a micropipette caliper. The hydrogel was placed in a constant-temperature incubator at 37 °C. At different time points, the number of colonies was counted by an automatic colony counting apparatus, and the distribution and growth of colonies were observed.

Bacterial Count Method. We took two identical grinding test tubes and mark them with numbers 1 and 2. We took 2 g of the hydrogel and cut it into granules with scissors. In test tube 1, 20 mL of bacterial culture fluid was measured from tubes 1 and 2, and the two tubes were placed in a constant-temperature oscillator (37 °C, 180 rpm), and the density of the bacteria in the test tube was measured at different time points with a handheld automatic cell counter at two. Finally, with eq. (2), the rate of bacterial reduction was calculated:

$$\text{Rate of bacterial reduction}(\%) = (B - A)/B \times 100\% \quad (2)$$

where B is the cell count of the control group and A is the cell count of the experimental group.

Cell Toxicity Test

Amounts of 2, 4, and 8 g of drying and mashed hydrogels were added to a 20 mL solution containing 10% fetal bovine serum 1640 culture medium and incubated at 37 °C with 5% CO_2; it was then extracted by 0.22 μm membrane filtration sterilization. To obtain the logarithmic growth period of the L929 cells, the cell concentration was adjusted to $1 \times 10^4\ mL^{-1}$, and then, we added the samples to the 96-well plate (each hole was 100 μL) and placed the plate in the box and incubated it for 24 h at 37 °C with 5% CO_2. A leaching solution of the hydrogel was added to 96-well plates (each hole was 100 μL). We set the control hole and complete medium control wells. The blank control hole had an equal volume of complete medium, and the complete medium control wells did not have cells. The final volume of each hole was 200 μL. Each group was divided into three complex holes and were then placed and incubated in the box for 24 h at 37 °C with 5% CO_2. A volume of 10 μL of Alamar Blue solution was added to each hole; when the medium color changed from blue cyan to pink, we detected the fluorescence

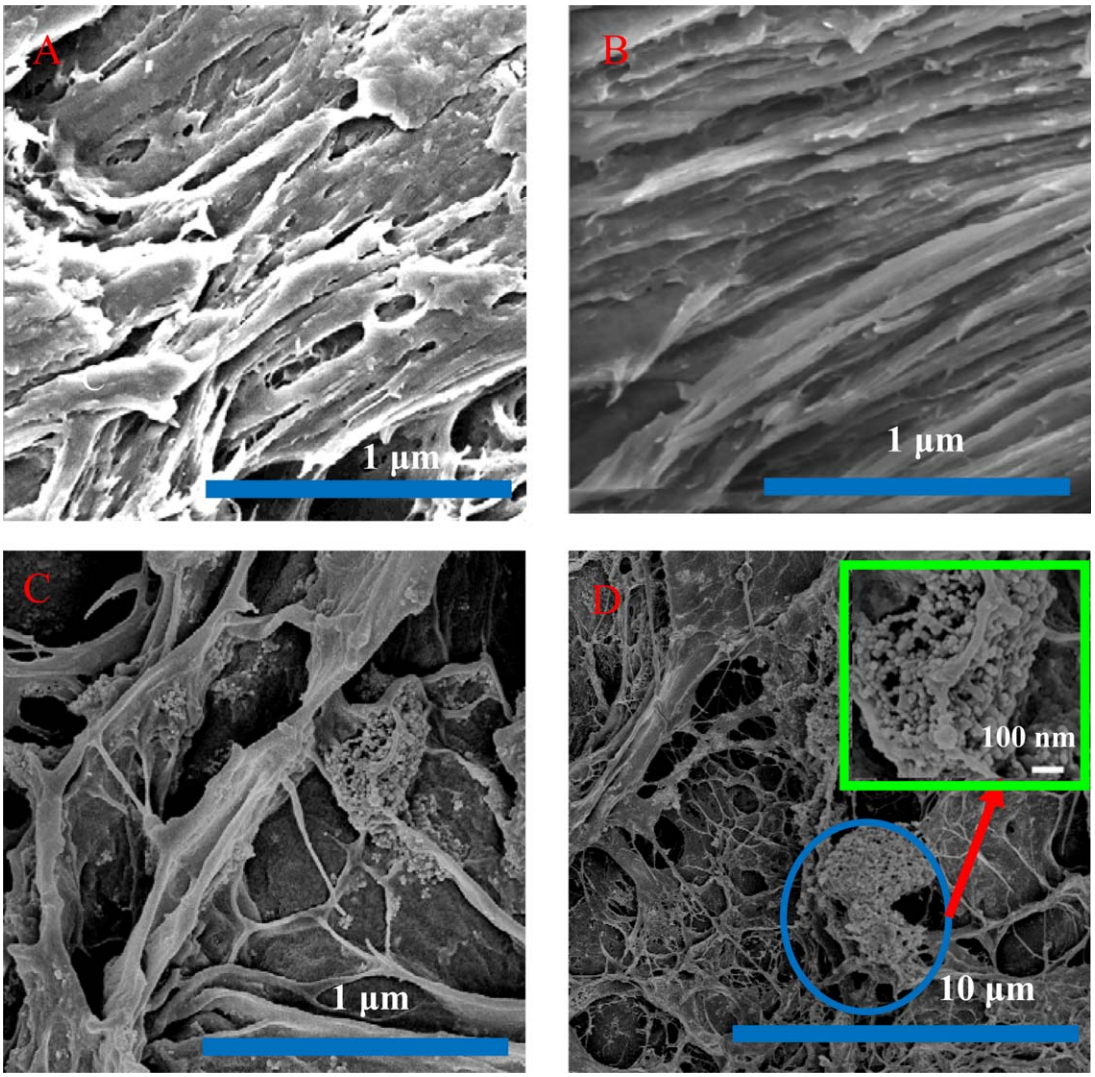

Figure 1. SEM and FESEM images of the TiO_2/CMCS/PVA composite hydrogel: (A) frontal and (B) side-view SEM images, (C) FESEM image, and (D) high-magnification image. [Color figure can be viewed in the online issue, which is available at wileyonlinelibrary.com.]

intensity of the samples with a spectrophotometric meter and calculated the Alamar Blue reduction rate.

RESULTS AND DISCUSSION

Micromorphology of the TiO_2/CMCS/PVA Nanocomposite Hydrogel

Figure 1 shows the micromorphology of the nano-TiO_2/CMCS/PVA ternary composite hydrogel. As shown in Figure 1(A), the white highlights may be the doped nano-TiO_2; the TiO_2 nanoparticles were further confirmed through FESEM [Figure 1(C,D)]. These nanomaterials were adsorbed into the hydrogel structural voids; this increased the swelling degree and mechanical properties of the hydrogel. The nanomaterials changed the surface structure of the hydrogel to fill the gaps; this improved the structure of the hydrogel surface, so the structure was smooth. Meanwhile, the surface effect of nano-TiO_2 greatly stimulated the activity of the surface of the hydrogel. When we further improved the resolution [Figure 1(B)], we observed that the skeleton of the hydrogel was regular, the distribution of the transverse hole was uniform, and the hole exhibited a horizontal plane and vertical disorder. So, the hydrogel had a good tensile strength, but the compressive strength was relatively poor. However, the hydrogel had a large internal porosity, and this made the hydrogel have a very strong swelling capacity. At the same time, the existence of the internal pores in the hydrogel resulted in a high surface area, and the great activity of the hydrogel will have great significance for its application in the field of smart hydrogels.

FTIR Analysis of the Nano-TiO_2/CMCS/PVA Ternary Composite Hydrogel

FTIR spectra of the TiO_2-loaded hydrogel samples containing different concentrations of TiO_2 (0.5, 1, 2, 3, 4, 5, and 6%) were also recorded to determine the variation in the interactions between CMCS, PVA, and TiO_2 (Figure 2). The major peaks were at 3275 cm^{-1} (O—H stretching), 2920 and 2852 cm^{-1} (C—H stretching), 1750 cm^{-1} (C—O stretching of PVA), 1417 cm^{-1} (O—H deformation), and 1244 cm^{-1} (C—O

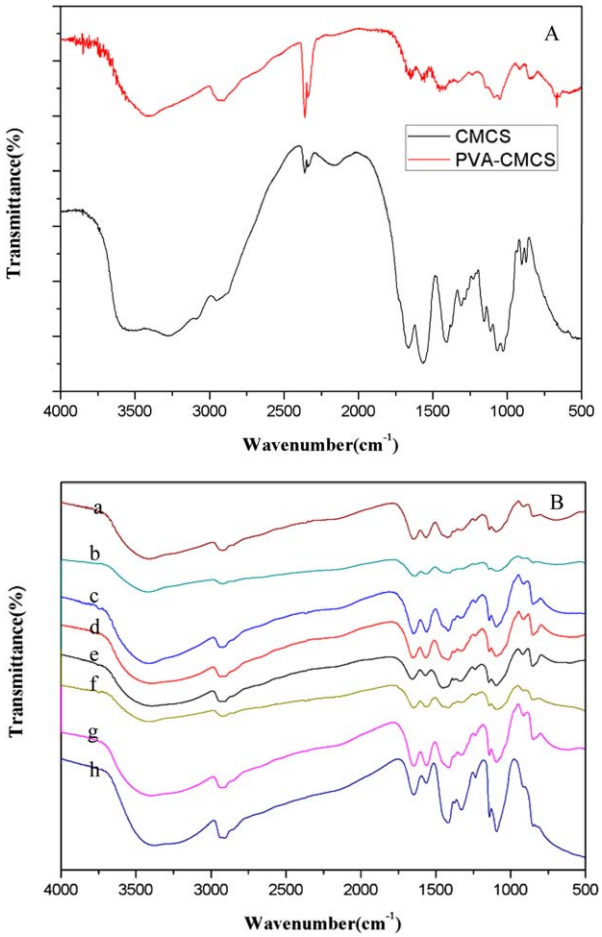

Figure 2. FTIR spectra of the TiO_2/CMCS/PVA hydrogels: (A) synthesized hydrogel without TiO_2 and (B) synthesized hydrogel with TiO_2 [(a) PVA–TiO_2, (b) CMCS–PVA–3% TiO_2, (c) CMCS–PVA–2% TiO_2, (d) CMCS–PVA–1% TiO_2, (e) CMCS–PVA–0.5% TiO_2, (f) CMCS–PVA–5% TiO_2, (g) CMCS–PVA–4% TiO_2, and (h) CMCS–PVA–6% TiO_2]. [Color figure can be viewed in the online issue, which is available at wileyonlinelibrary.com.]

stretching of PVA); peaks at 960–400 cm^{-1} were the characteristic vibrational modes for TiO_2 (Ti—O). In the spectrum of the CMCS group, the strong peaks at 3433.26 and 1086.76 cm^{-1} were assigned to the —OH stretching of adsorbed bound water and the —NH_2 absorption peak, respectively. In the spectrum of the PVA group, the strong characteristic peaks of —OH at 3338 and 1422 cm^{-1} were assigned to the —OH stretching vibrations and CH—OH bending vibrations. After the PVA was compounded with CMCS, the hydrogen bond force between the molecules was reduced, and the characteristic peak at 3338 cm^{-1} weakened significantly. This new generation of chemical bonds and the retention of original functional groups could be useful for TiO_2/CMCS/PVA ternary composite hydrogels to retain a high antibacterial activity.

TG Analysis of the Nano-TiO_2/CMCS/PVA Ternary Composite Hydrogel

The thermal stability of the TiO_2-loaded hydrogels containing different concentrations of TiO_2 (0.5, 1, 2, 3, 4, 5, and 6%) was

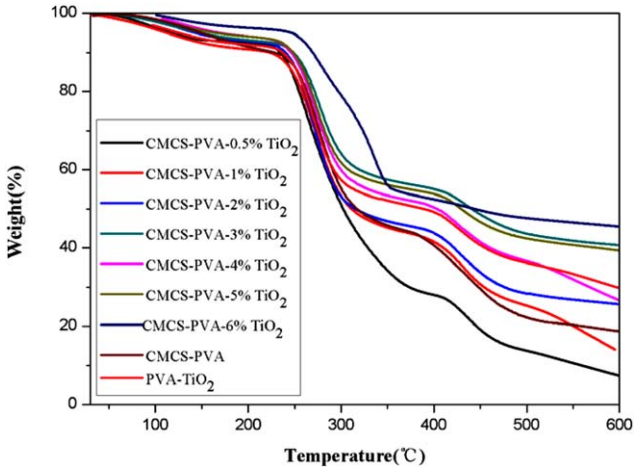

Figure 3. TG analysis of the TiO_2/CMCS/PVA hydrogels. [Color figure can be viewed in the online issue, which is available at wileyonlinelibrary.com.]

determined by TG analysis. Figure 3 shows the thermogram of TiO_2-loaded and unloaded dry hydrogel samples; the weight loss rate was slow and represented only water evaporation from room temperature to 210 °C. However, the weight loss rate was accelerated at 210–500 °C; this indicated that the temperature accelerated the decomposition of CMCS and PVA after 210 °C. In the melting process, the CMCS and PVA decomposed; this was the reason why melt processing was difficult. Beyond 500 °C, the CMCS and PVA was completely decomposed and carbonized. Because there was good compatibility between PVA and other macromolecules, there were no significant differences on the TG analysis curve of the single-component PVA and the CMCS/PVA crosslinked composite polymer. Overall, the weight loss was lower when the content of TiO_2 was increased. According to the preparation of the experiment, the results may also be helpful for TiO_2/CMCS/PVA hydrogels to obtain better antibacterial properties.

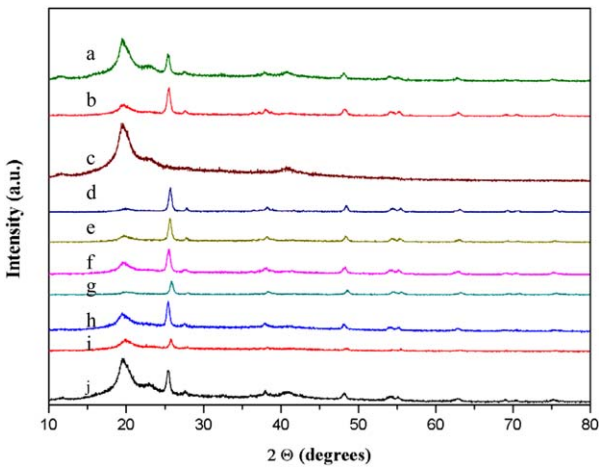

Figure 4. XRD patterns of the TiO_2/CMCS/PVA hydrogels: (a) CMCS–PVA–TiO_2, (b) PVA–TiO_2, (c) PVA–CMCS, (d) CMCS–PVA–6% TiO_2, (e) CMCS–PVA–5% TiO_2, (f) CMCS–PVA–4% TiO_2, (g) CMCS–PVA–3% TiO_2, (h) CMCS–PVA–2% TiO_2, (i) CMCS–PVA–1% TiO_2, and (j) CMCS–PVA–0.5% TiO_2. [Color figure can be viewed in the online issue, which is available at wileyonlinelibrary.com.]

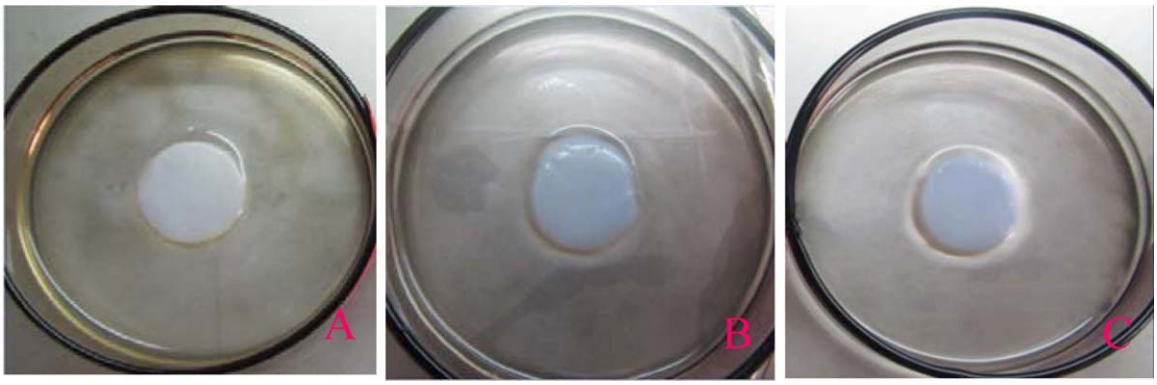

Figure 5. Images of the antibacterial circles of different hydrogels against *E. coli*: (A) pure PVA, (B) TiO_2/PVA nanocomposite hydrogel, and (C) TiO_2/CMCS/PVA nanocomposite hydrogel. [Color figure can be viewed in the online issue, which is available at wileyonlinelibrary.com.]

XRD Analysis of the Nano-TiO_2/CMCS/PVA Ternary Composite Hydrogel

The typical powder XRD pattern of the ternary composite hydrogels containing different concentrations of TiO_2 (0.5, 1, 2, 3, 4, 5, and 6%) is shown in Figure 4. CMCS showed narrow bands at a 2θ of 20°; this demonstrated its crystalline structure. The XRD diffraction peaks around 2θs of 25.2, 37.9, 47.8, and 55.0°, which could be indexed to the characteristic peaks (101), (004), (200), and (201) of anatase TiO_2, and the peaks around 2θs of 27.42, 36.10, and 41.24° could be indexed to the characteristic peaks (101), (004), and (200) of rutile TiO_2. The XRD diffraction peaks of TiO_2 did not change significantly after TiO_2 was loaded into the composite hydrogel, especially TiO_2/CMCS/PVA. The hydrogel had an appropriate peak width and peak height at concentrations of TiO_2 (5%). Perhaps it had a certain impact on the antibacterial performance, whereas in the CMCS diffraction peaks of the TiO_2/CMCS/PVA hydrogel almost disappeared with increasing of the TiO_2 content. These results indicate that the original crystalline structure of CMCS altered after complexation with TiO_2.

Determination of the Antibacterial Properties of the Hydrogels

Antibacterial Circle Method. As shown in Figure 5, we observed that the pure PVA hydrogel was still a transparent liquid and did not form the antibacterial circle [Figure 5(A)], whereas the two TiO_2/PVA composite hydrogels had certain antibacterial circles [Figure 5(B)]. The TiO_2/CMCS/PVA composite hydrogel was very obvious around the white fungus

Table 1. Diameters of the Antibacterial Circles of the Pure PVA, CMCS/PVA Composite Hydrogel, TiO_2/PVA Nanocomposite Hydrogel, and TiO_2/CMCS/PVA Nanocomposite Hydrogel against *E. coli* and *S. aureus*

	Antibacterial circle diameter (mm)							
	E. coli				*S. aureus*			
Hydrogel	1	2	3	Average diameter	1	2	3	Average diameter
PVA	0	0	0	0	0	0	0	0
CMCS/PVA	2.46	2.23	2.16	2.28	2.74	2.60	2.58	2.64
TiO_2/PVA	2.86	3.04	2.90	2.93	2.71	2.81	2.85	2.79
TiO_2/CMCS/PVA	4.10	4.18	4.30	4.19	4.18	4.54	4.34	4.35

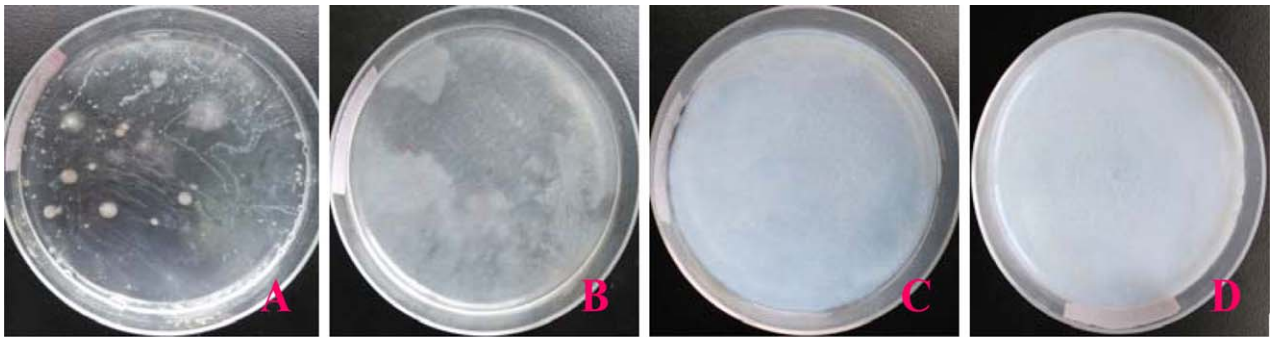

Figure 6. Images of bacterial colony distributions of different hydrogels on *E. coli*: (A) pure PVA, (B) CMCS/PVA, (C) TiO_2/PVA, and (D) TiO_2/CMCS/PVA. [Color figure can be viewed in the online issue, which is available at wileyonlinelibrary.com.]

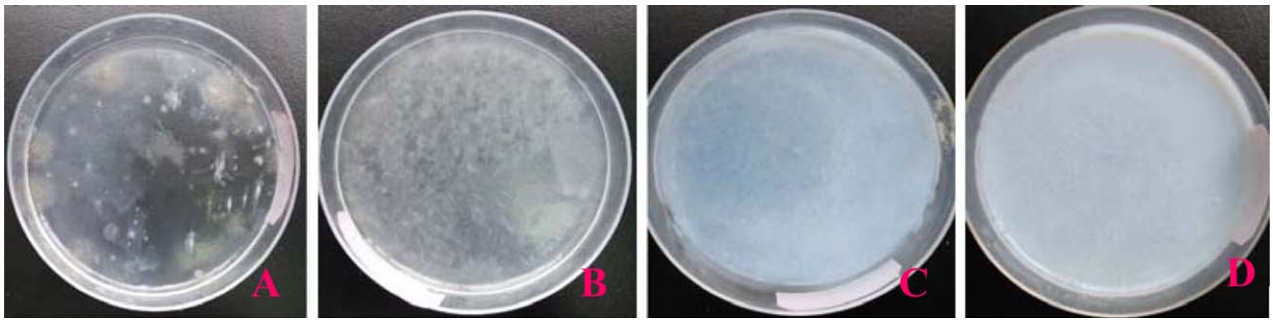

Figure 7. Images of bacterial colony distributions of different hydrogels on *S. aureus*: (A) pure PVA, (B) CMCS/PVA, (C) TiO_2/PVA, and (D) TiO_2/CMCS/PVA. [Color figure can be viewed in the online issue, which is available at wileyonlinelibrary.com.]

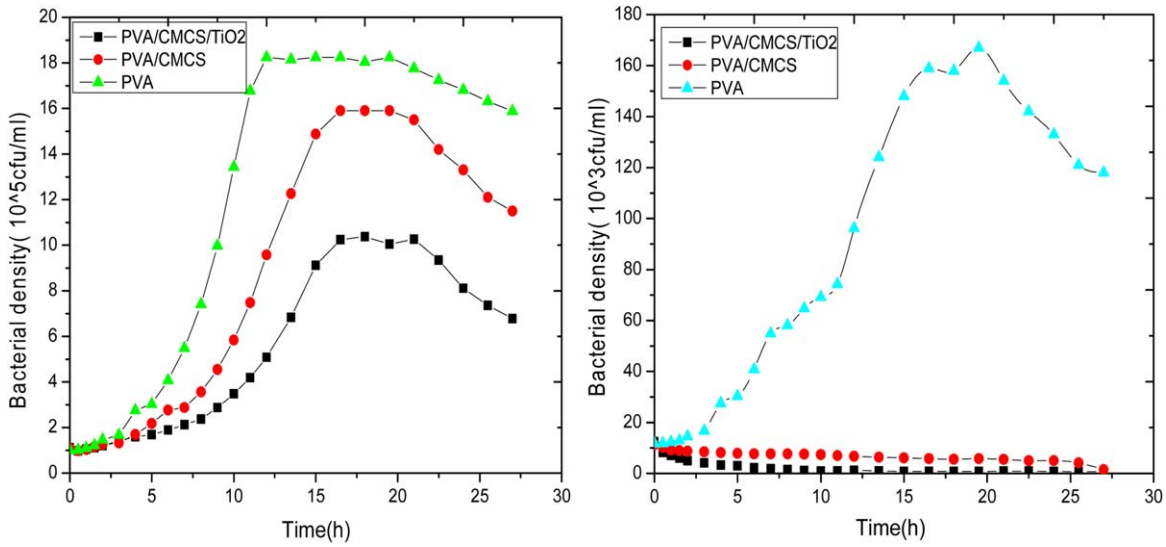

Figure 8. Curves of the bacterial density on different hydrogels against *E. coli* (left) and *S. aureus* (right). [Color figure can be viewed in the online issue, which is available at wileyonlinelibrary.com.]

[Figure 5(C)]. Through the comparison of several groups of different types of hydrogel antibacterial effect against *E. coli* and *S. aureus*, the results show that the pure PVA did not form the antibacterial circle and the two CMCS/PVA composite hydrogels had antibacterial circles. The average antibacterial circle diameters were 2.28 and 2.64 mm, respectively (Table 1). However, the two TiO_2/PVA composite hydrogel circles had diameters of 2.93 and 2.79 mm, respectively; those of the TiO_2/CMCS/PVA composite hydrogels were 4.19 and 4.35 mm. These results suggest that nano-TiO_2 composite hydrogel had the strongest antibacterial activity, possibly because with the introduction of nano-TiO_2, the surface structure and morphology of the CMCS/PVA composite hydrogel were changed. This resulted in a synergistic effect.

Plate Count Method. Figures 6 and 7 present the colony culture for several groups of different types of hydrogels for *E. coli* and *S. aureus*. The results show a large number of colonies on the surface of the pure PVA hydrogel [Figures 6(A) and 7(A)]; this further confirmed that the pure PVA hydrogel did not have antibacterial activity. The CMCS/PVA composite hydrogel [Figures 6(B) and 7(B)] had a certain inhibition for the size and number of colonies. The effect may have been due to CMCS; this gave the CMCS/PVA composite hydrogel a certain antibacterial activity. However, the TiO_2/PVA and TiO_2/CMCS/PVA composite hydrogel did not form the obvious *E. coli* colonies

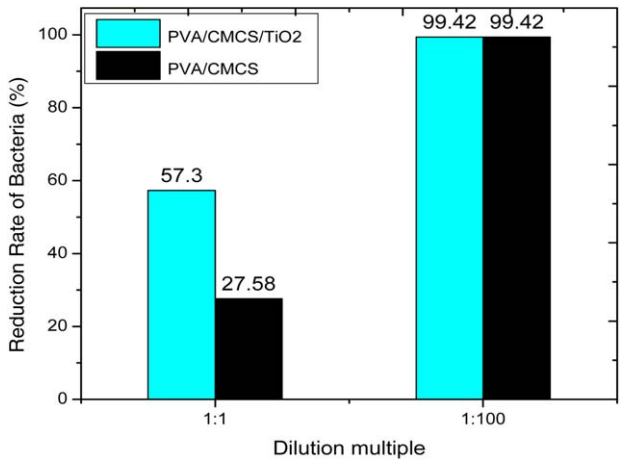

Figure 9. Antibacterial properties of the CMCS/PVA hydrogel and the TiO_2/CMCS/PVA hydrogel against *E. coli* at different dilution concentrations. [Color figure can be viewed in the online issue, which is available at wileyonlinelibrary.com.]

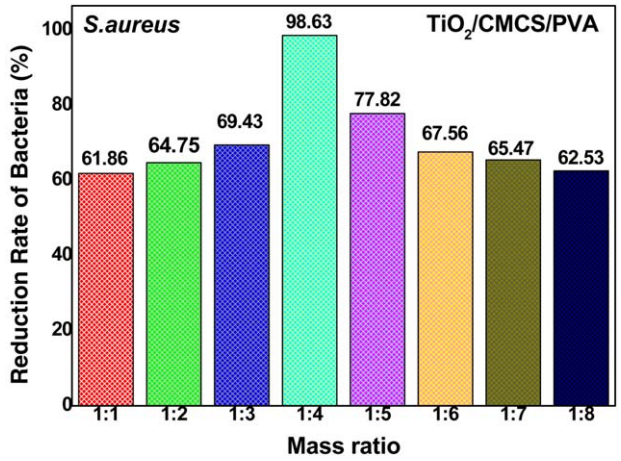

Figure 10. Antibacterial properties of the TiO_2/CMCS/PVA hydrogels against *S. aureus* at different mass ratios of CMCS and PVA ([TiO_2] = 5%; dilution ratio of *S. aureus* = 1:100; CMCS:PVA mass ratio = 1:1, 1:2, 1:3, 1:4, 1:5, 1:6, 1:7, or 1:8). [Color figure can be viewed in the online issue, which is available at wileyonlinelibrary.com.]

because of the introduction of nano-TiO_2; the microstructure of the composite hydrogel was changed, and the synergistic antibacterial effect of nano-TiO_2 and CMCS was formed.

Bacterial Count Method. We evaluated the effect of the hydrogel on the growth curve of *E. coli* and *S. aureus* (as shown in Figure 8) under the condition of the culture medium with different hydrogels. The analysis showed that the growth process of *E. coli* experienced four characteristic stages: a slow-growth lag phase, a logarithmic phase of rapid growth, a relatively stable stationary phase, and a declining phase. The growth curves of three kinds of different hydrogels on *E. coli* were compared. The results show that the antibacterial effect of TiO_2/CMCS/PVA composite hydrogel was the best, and the results were consistent with previous results. With the same method, we evaluated the antibacterial effects of three kinds of different hydrogels on *S. aureus*. The results show that the addition of the TiO_2/CMCS/PVA composite hydrogel had a significant effect on the growth curve of *S. aureus* and almost completely inhibited the growth of the bacteria.

To further explore the antibacterial properties of the TiO_2/CMCS/PVA composite hydrogel against the low-density bacteria, we studied the antibacterial properties of the CMCS/PVA and TiO_2/CMCS/PVA composite hydrogels against low-density *E. coli* with different dilution multiples.

Figure 9 shows that when the dilution ratio of *E. coli* (the initial concentration was about 10^6 cells/mL) was 1:1, the antibacterial rate (57.3%) of the TiO_2/CMCS/PVA composite hydrogel was higher than that of CMCS/PVA (27.58%); when the dilution ratio of *E. coli* was 1:100. Both of the antibacterial rates (99.42%) were obviously improved. At the same time, we indicated that although the different hydrogels had very strong

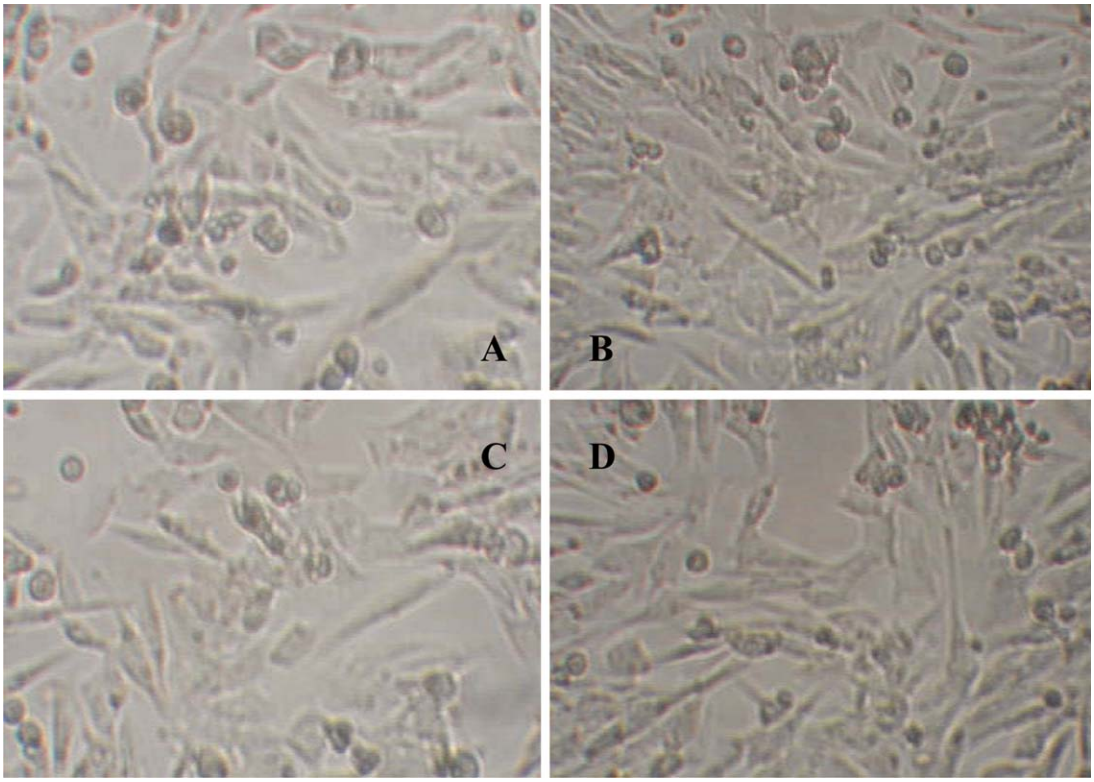

Figure 11. Images of the cell growth of L929 with the addition of leaching solutions of different hydrogels (100×): (A) before and (b) after without the addition of a leaching solution of a hydrogel and (C) before and (D) after with the addition of a leaching solution of the TiO_2/CMCS/PVA hydrogel. [Color figure can be viewed in the online issue, which is available at wileyonlinelibrary.com.]

Table 2. Effects of Different Leaching Solution Concentrations of the Hydrogels on L929 Cell Activity

Hydrogel sample	Alamar Blue reduction ratio (%)		
	0.1 g/mL	0.2 g/mL	0.4 g/mL
Control	75.82 ± 4.32	75.82 ± 4.32	75.82 ± 4.32
PVA	75.18 ± 2.74	73.93 ± 4.01	72.06 ± 1.55
CMCS/PVA	75.38 ± 3.54	74.99 ± 4.77	71.28 ± 3.51
TiO_2/CMCS/PVA	73.41 ± 2.64	72.36 ± 3.42	71.41 ± 2.17

inhibition effects on the growth of bacteria, but the difference in the antibacterial properties was obviously weakened under the conditions of an extremely dilute concentration of bacteria.

To understand the antibacterial properties of the TiO_2/CMCS/PVA hydrogel on *S. aureus* at different mass ratios of CMCS and PVA, eight hydrogels with different mass ratios of CMCS and PVA (viz., 1:1, 1:2, 1:3, 1:4, 1:5, 1:6, 1:7, and 1:8) are shown in Figure 10. The trend of antibacterial rate was first increased and then decreased gradually with the increasing mass ratio of CMCS to PVA; the maximum antibacterial rate (98.63%) appeared when the mass ratio of CMCS and PVA was 1:4. This showed that the constituents of CMCS in the composite hydrogel played an important role in the antibacterial process; after the mass ratio of CMCS was introduced, different swelling degrees, gel fractions, crosslinking degrees and network structures of the nanocomposite hydrogels were obtained, and these possibly contributed to the improvement of the antibacterial properties of the TiO_2/CMCS/PVA hydrogel on *S. aureus*.

Antibacterial Mechanism of the Nano-TiO_2/CMCS/PVA Composite Hydrogels

Through the experimental analysis, we found that the TiO_2/CMCS/PVA composite hydrogels had good antibacterial activity. The antibacterial mechanism could be attributed to several aspects. First, CMCS was placed with the protonated ammonium at the time of deacetylation; the interaction between protonated ammonium and the bacteria cell membrane with negative charge, the adsorption and accumulation of bacteria, and the penetration of the cell wall into the cell disrupted the bacterial metabolism and synthesis.[35,36] Second, CMCS introduced, the negative charge distribution on the cell membrane, and the cell wall were not uniform; this resulted in the dissolution of the cell wall; this played a role in killing bacteria.[37] Third, the probably free radicals, which were derived from the surface of the nano-TiO_2, acted on the cell membrane phospholipid layer, and destroyed the bacterial cell membrane to increase the permeability of the cell membrane; at the same time, it caused the cell membrane permeability change and caused cell swelling. The final result was cell death.[38,39]

In a word, the excellent antibacterial effect of TiO_2/CMCS/PVA composite hydrogel was mainly due to the synergistic effect of several kinds of different antibacterial materials.

Evaluation of the Toxicity of the Hydrogel by the Alamar Blue Method

Alamar Blue is a redox indicator under the condition of oxidation and is a nonfluorescent blue purple. In the reduction state, it was transformed into a reduction product of pink or red fluorescence to indicate the metabolic activity of cells.[40,41] In the process of cell proliferation, the intracellular area is in a reducing environment, and Alamar Blue is released to the cell and dissolved in the culture medium after the reduction so that the culture medium is revealed. The fluorescence intensity was proportional to the number of active cells, and the reduction rate of Alamar Blue was calculated by the fluorescence value; this reflected the cell activity and the interference factor to the cell's toxicity.

Table 2 shows that the data of different concentrations of different hydrogels on the activity of the L929 cells. With increasing concentration of three kinds of hydrogel extracts (from 0.1 to 0.4 g/mL), there was no significant effect on the reduction of Alamar Blue, and this suggested that three kinds of different hydrogels had no obvious cytotoxicity on the L929 cells. The effects of different hydrogel extracts on the morphology of the L929 cells were observed (Figure 11), and the experimental results confirmed that the nano-TiO_2/CMCS/PVA composite hydrogel had no obvious toxicity on the L929 cells and complied the requirements for the safety of biological materials.[42]

CONCLUSIONS

The nano-TiO_2/CMCS/PVA composite hydrogel was prepared by freezing–thawing cycle method and an electron-beam radiation technique. With *E. coli* and *S. aureus* as bacterial models, the antibacterial activity were demonstrated by the antibacterial circle method, plate count method, and cell density method. The results show that the antibacterial activities of the TiO_2/CMCS/PVA hydrogel against *E. coli* and *S. aureus* were better than those of single-component PVA hydrogel and CMCS/PVA composite hydrogel. The composition of the polymer and its structure and nano-TiO_2 contributed to the micromorphology and surface structure of the composite hydrogel; the synergistic effect between nano-TiO_2 and the polymer and so on likely contributed to the improvement of the antibacterial performance. An Alamar Blue assay was used to study the cytotoxicity of the composite hydrogel on the fibroblast cell line L929. The results show that the reduction rate of Alamar Blue was not significantly affected by the different concentrations of TiO_2/CMCS/PVA, and there was no significant cytotoxicity to the L929 cells. This new type of photosensitive antibacterial hydrogel is expected to be a comprehensive balance of the polymer and nano-inorganic material components of the performance. This eliminated a single component of the weaknesses and allowed us to obtain a more comprehensive performance in the

composite hydrogel antibacterial materials for effective application in cosmetics, medical dressings, environmental protection, and other fields.

ACKNOWLEDGMENTS

This work was supported by the National Natural Science Foundation of China (contract grant numbers 11405050 and 8100704), the Key Projects of the Education Department of Hubei Province (contract grant number D20142804), the National University Students Training and Entrepreneurial Practice Project (contract grant numbers 201210927033 and 20131092723), and the 12th Five-Year Plan of Hubei Province (contract grant number 2014B243).

REFERENCES

1. Peppas, N. A.; Bures, P.; Leobandung, W.; Ichikawa, H. *Eur. J. Pharm. Biopharm.* **2000**, *50*, 27.
2. Rattanaruengsrikul, V.; Pimpha, N.; Supaphol, P. *Macromol. Biosci.* **2009**, *9*, 1004.
3. Ma, D.; Cai, X.; Lin, Q. M.; Zhang, J. L.; Mai, W. J.; Tan, S. Z.; Xue, W.; Wu, T. *J. Appl. Polym. Sci.* **2013**, *130*, 1554.
4. Rattanaruengsrikul, V.; Pimpha, N.; Supaphol, P. *J. Appl. Polym. Sci.* **2012**, *124*, 1668.
5. Bajpai, S. K.; Chand, N.; Mahendra, M. *Polym. Eng. Sci.* **2013**, *53*, 1751.
6. Varaprasad, K.; Mohan, Y. M.; Vimala, K.; Mohana Raju, K. *J. Appl. Polym. Sci.* **2011**, *121*, 784.
7. Valle, H.; Rivas, B. L.; Fernandez, M.; Mondaca, M. A.; Aguilar, M. R.; San Roman, J. *J. Appl. Polym. Sci.* **2014**, *131*, DOI: 10.1002/app.39644.
8. Liu, T.; Wu, T.; Liu, H. X.; Ke, B.; Huang, H. X.; Jiang, Z. Y.; Xie, M. Q. *J. Appl. Polym. Sci.* **2014**, *131*, 4525.
9. Li, H. N.; Yang, J.; Hu, X. N.; Liang, J.; Fan, Y. J.; Zhang, X. D. *J. Biomed. Mater. Res. Part A* **2011**, *98*, 31.
10. Chatelet, C.; Damour, O.; Domard, A. *Biomaterials* **2001**, *22*, 261.
11. Upadhyaya, L.; Singh, J.; Agarwal, V.; Tewari, R. P. *J. Controlled Release* **2014**, *186*, 54.
12. Mi, F. L.; Wu, Y. B.; Shyu, S. S.; Chao, A. C.; Lai, J. Y.; Su, C. C. J. *Membr. Sci.* **2003**, *212*, 237.
13. Wu, F.; Meng, G.; He, J.; Wu, Y.; Wu, F.; Gu, Z. *ACS Appl. Mater. Interfaces* **2014**, *6*, 10005.
14. Liu, B.; Hu, J.; Meng, Q. J. *Biomed. Mater. Res. Part B* **2009**, *89*, 1.
15. Tsao, C. T.; Chang, C. H.; Lin, Y. Y.; Wu, M. F.; Wang, J. L.; Han, J. L.; Hsieh, K. H. *Carbohydr. Res.* **2010**, *345*, 1774.
16. Ding, F.; Nie, Z.; Deng, H.; Xiao, L.; Du, Y.; Shi, X. *Carbohydr. Polym.* **2013**, *98*, 1547.
17. Radhakumary, C.; Antonty, M.; Sreenivasan, K. *Carbohydr. Polym.* **2011**, *83*, 705.
18. Vimala, K.; Mohan, Y. M.; Sivudu, K. S.; Varaprasad, K.; Ravindra, S.; Reddy, N. N.; Padma, Y.; Sreedhar, B.; Mohanaraju, K. *Colloids Surf. B* **2010**, *76*, 248.
19. Chen, Y. F.; Yi, M. *Acta Polym. Sin.* **2001**, 1, 215.
20. Koosha, M.; Mirzadeh, H.; Shokrgozar, M. A.; Farokhi, M. *RSC Adv.* **2015**, *5*, 10479.
21. Lad, U.; Kale, G. M.; Bryaskova, R. *Anal. Chem.* **2013**, *85*, 6349.
22. Juby, K. A.; Dwivedi, C.; Kumar, M.; Kota, S.; Misra, H. S.; Bajaj, P. N. *Carbohydr. Polym.* **2012**, *89*, 906.
23. Varaprasad, K.; Mohan, Y. M.; Ravindra, S.; Reddy, N. N.; Vimala, K.; Monika, K.; Sreedhar, B.; Raju, K. M. *J. Appl. Polym. Sci.* **2010**, *115*, 1199.
24. Garcia-Contreras, R.; Scougall-Vilchis, R. J.; Contreras-Bulnes, R.; Sakagami, H.; Morales-Luckie, R. A.; Nakajima, H. *J. Appl. Oral. Sci.* **2015**, *23*, 321.
25. Mungkalasiri, J.; Bedel, L.; Emieux, F.; Dore, J.; Renaud, F. N. R.; Sarantopoulos, C.; Maury, F. *Chem. Vapor Deposition* **2010**, *16*, 35.
26. Kim, S. W.; An, Y. *J. Appl. Microbiol. Biotechnol.* **2012**, *95*, 243.
27. Kubacka, A.; Serrano, C.; Ferrer, M.; Lunsdorf, H.; Bielecki, P.; Cerrada, M. L.; Fernandez-Garcia, M. *Nano Lett.* **2007**, *7*, 2529.
28. Carre, G.; Hamon, E.; Ennahar, S.; Estner, M.; Lett, M. C.; Horvatovich, P.; Gies, J. P.; Keller, V.; Keller, N.; Andre, P. *Appl. Environ. Microbiol.* **2014**, *80*, 2573.
29. Lydakis-Simantiris, N.; Riga, D.; Katsivela, E.; Mantzavinos, D.; Xekoukoulotakis, N. P. *Desalination* **2010**, *250*, 351.
30. Li, Y. S.; Zhang, Y.; Sun, S. F.; Zhang, A. Q.; Liu, Y. *J. Photochem. Photobiol. B* **2013**, *128*, 12.
31. Young, S. K. *Mater. Res. Soc.* **2010**, *93*, 120.
32. Du, Y. M.; Wen, Y.; Li, Z. *J. Wuhan Univ. Nat. Sci. Ed.* **2002**, *48*, 701.
33. Du, Y. M.; Dong, Z. F.; Fan, L. H.; Wen, Y.; Liu, H.; Wang, X. H. *J. Funct. Polym.* **2004**, *17*, 61.
34. Schwartz, V. B.; Thétiot, F.; Ritz, S.; Pütz, S.; Choritz, L.; Lappas, A.; Förch, R.; Landfester, K.; Jonas, U. *Adv. Funct. Mater.* **2012**, *22*, 2376.
35. Sahiner, N. *Prog. Polym. Sci.* **2013**, *38*, 1329.
36. Tang, H. W.; Chen, G. Q.; Zhou, J. S.; Wu, Q. S. *Anal. Chim. Acta* **2002**, *468*, 27.
37. Amezaga-Madrid, P.; Silveyra-Morales, R.; Cordoba-Fierro, L.; Nevarez-Moorillon, G. V.; Miki-Yoshida, M.; Orrantia-Borunda, E.; Solis, F. J. *J. Photochem. Photobiol. B* **2003**, *70*, 45.
38. Vacaroiu, C.; Enache, M.; Gartner, M.; Popescu, G.; Anastasescu, M.; Brezeanu, A.; Todorova, N.; Giannakopoulou, T.; Trapalis, C.; Dumitru, L. *World J. Microbiol. Biotechnol.* **2009**, *25*, 27.
39. Kikuchi, Y.; Sunada, K.; Iyoda, T.; Hashimoto, K.; Fujishima, A. J. *Photochem. Photobiol. A* **1997**, *106*, 51.
40. Rampersad, S. N. *Sensors* **2012**, *12*, 12347.
41. Vega-Avila, E.; Pugsley, M. K. *Proc. West. Pharmacol. Soc.* **2011**, *54*, 10.
42. Bi, S. X.; Yang, N.; Yang, M. K.; He, X. L.; Zhang, Q. S.; Chen, L.; Zhu, Z. Y.; Gao, Y. T.; Du, Z. *Acta Polym. Sin.* **2013**, 0, 888.